Conformational propensity and biological studies of proline mutated LR peptides inhibiting human thymidylate synthase and ovarian cancer cell growth.

Journal:	*Journal of Medicinal Chemistry*
Manuscript ID	jm-2017-01699h.R2
Manuscript Type:	Brief Article
Date Submitted by the Author:	n/a
Complete List of Authors:	Saxena, Puneet; University of Modena and Reggio Emilia, Department Life Science; Excelra Knowledge Solutions Pvt. Ltd. Severi, Leda; University of Modena and Reggio Emilia, Department of Life Science Santucci, Matteo; Modena and Reggio Emilia University, Department of Life Science Taddia, Laura; University of Modena and Reggio Emilia, Department of Life Science Ferrari, Stefania; Università degli Studi di Modena e Reggio Emilia, Department of Life Science Luciani, Rosaria; University of Modena and Reggio Emilia, Department of Life Science Marverti, Gaetano; University of Modena and reggio Emilia, Department of Biomedical Science Marraccini, Chiara; Universita Di Modena e Reggio Emilia, Department of Life Science Tondi, Donatella; Università di Modena e Reggio Emilia, Department of Life Sciences Mor, Marco; Universita degli Studi di Parma, Dipartimento di Farmacia Scalvini, Laura; University of Parma, Food and Drug Department Vitiello, Simone; University of Modena and Reggio Emilia, Life Science Losi, Lorena; Universita Di Modena e Reggio Emilia, Department of Life Science; Pathological Anatomy Fonda, Sergio; Universita Di Modena e Reggio Emilia, Department of Life Science Pacifico, Salvatore; Università degli Studi di Ferrara, Dipartimento di Scienze Chimiche e Farmaceutiche Guerrini, Remo; Università degli Studi di Ferrara, Dipartimento di Scienze Chimiche e Farmaceutiche D'Arca, Domenico; Universita degli Studi di Modena e Reggio Emilia Dipartimento di Scienze Biomediche Metaboliche e Neuroscienze Ponterini, Glauco; Università di Modena e Reggio Emilia, Department of Life Science Costi, Maria Paola; University of Modena and Reggio Emilia, Department of Life Science

Conformational propensity and biological studies of proline mutated LR peptides inhibiting human thymidylate synthase and ovarian cancer cell growth.

Puneet Saxena,[‡,#] Leda Severi[‡], Matteo Santucci[‡], Laura Taddia[‡], Stefania Ferrari[‡], Rosaria Luciani[‡], Gaetano Marverti[§], Chiara Marraccini[‡$], Donatella Tondi[‡], Marco Mor[^], Laura Scalvini[^], Simone Vitiello[‡], Lorena Losi[‡±], Sergio Fonda[‡], Salvatore Pacifico[†], Remo Guerrini[†⊥], Domenico D'Arca[§], Glauco Ponterini[‡*] and Maria Paola Costi[‡*]

[‡]Department of Life Sciences, University of Modena and Reggio Emilia, via Campi, 103, 41125 Modena, Italy.
[§]Department of Biomedical Sciences, Metabolic and Neural Sciences, University of Modena and Reggio Emilia, via Campi 287, 41125 Modena, Italy.
[^] Dipartimento di Scienze degli Alimenti e del Farmaco, Università di Parma, Parco Area delle Scienze 27/A , I-43124 Parma , Italy.
[±]Pathological Anatomy, via del Pozzo 71, 41124 Modena, Italy.
[†]Department of Chemical and Pharmaceutical Sciences, University of Ferrara, via Luigi Borsari 46, 44121 Ferrara, Italy.
[⊥]LTTA (Laboratorio per le Tecnologie delle Terapie Avanzate), via Fossato di Mortara 17-19, 44100 Ferrara, Italy.

KEYWORDS: peptide inhibitors, thymidylate synthase, ovarian cancer, protein expression modulation, conformational analysis.

ABSTRACT: LR and **[D-Gln^4]LR** peptides bind the monomer-monomer interface of human thymidylate synthase and inhibit cancer cell growth. Here, proline-mutated LR peptides were synthesized. Molecular dynamics calculations and circular dichroism spectra have provided a consistent picture of the conformational propensities of the [Pro^n]-peptides. **[Pro^3]LR** and **[Pro^4]LR** show improved cell growth inhibition and similar intracellular protein modulation than **LR**. These represent a step forward to the identification of more rigid and metabolically stable peptides.

INTRODUCTION

Human thymidylate synthase (hTS) is a homodimeric protein involved in the folate metabolic pathway. In its active form, hTS converts 2'-deoxyuridine-5'-monophosphate (dUMP) to 2'-deoxythymidine-5'-monophosphate (dTMP) in the presence of the cofactor N5,N10-methylentetrahydrofolate (mTHF). hTS also regulates protein synthesis, by interacting with its own as well as with the mRNAs of other proteins involved in the cell cycle.[1–4] This observation has made hTS an important drug target for fighting cancer.[5–7] However, prolonged dosage of clinically approved drugs such as 5-fluorouracil (**5FU,** prodrug of 5-fluoro-2'-deoxyuridine-5'-monophosphate), raltitrexed[8] and pemetrexed (**PMX**)[9], folate-cofactor analogs, leads to hTS overexpression, resulting in drug resistance.[10] To prevent and combat such resistance mechanism, drugs with new modes of action are needed.

The design of peptides mimicking portions of interfacial regions in the assemblies of multimeric proteins has led to the identification of inhibitors binding at the protein-protein interfaces.[11–14] Following this concept, we have previously synthesized a series of peptides derived from the parent **C20** peptide, a sequence coming from the monomer-monomer interface region of hTS (Figure 1). Our approach has resulted in the discovery of the lead **LR** peptide and its diastereomer **[D-Gln4]LR** acting with an allosteric inhibition profile against homodimeric hTS, engaging the protein in the cellular environment and leading to cancer cell growth inhibition without increasing hTS levels.[15,16] Mass spectrometric proteomic studies on cancer cells with the mentioned peptides have led to the identification of a panel of proteins, namely TS, dihydrofolate reductase (DHFR), heat shock protein HSP 90-alpha (HSP90), mitochondrial heat shock protein 75 kDa (TRAP1), bifunctional purine biosynthesis protein PURH (ATIC) and trifunctional purine biosynthetic protein adenosine-3 (GART), whose modulation is associated with the peptidic inhibitors activity.[17] Clinically approved drugs and peptidic inhibitors share a common target, hTS, but they show different effects on the proteomic profiles of cancer cells. The modulation of the protein panel so far identified can be considered a marker of the intracellular effects these peptides exert.[17]

The crystal structures of the complexes of hTS with two peptides, **LR** (PDBid: 3N5E) and **CQLYQRSG** (PDBid: 4FGT), confirm their binding at the monomer-monomer interface of hTS interacting with the Ala181-Ala197 loop (sequence residue numbers are taken from 4FGT) in the inactive form.[18] In these complexes, the peptides adopt folded, helical-type conformations, a finding further confirmed by circular dichroism (CD) and molecular dynamics (MD) simulation experiments.[19] With respect to the parent peptide, **LR**, **[D-Gln4]LR,** presents

enhanced rigidity, a tendency to assume an α-helical conformation and a stronger cellular growth inhibition.

With the aim to move towards more rigid peptides maintaining this mechanism of inhibition at the biochemical and cellular levels, we have performed the proline scanning of the **LR** peptide and have investigated the conformational preferences of the mutants by a combined experimental and computational approach based on CD spectroscopy and MD. It is well known that tumors express higher TS levels than normal tissues and that ovarian tissue is among those with the highest levels of TS expression.[20] An enhanced expression of the TS cycle has been associated with cross-resistance to 5-fluorouracil (5-FU) and methotrexate (MTX) in cisplatin-resistant human ovarian carcinoma cell lines.[21-24] and in other tumour types after cisplatin-based chemotherapy. [25,26] Therefore, the inhibition profile of these LR peptide derivatives against recombinant hTS as well as their activity at the cellular level against ovarian cancer cells has been evaluated. These peptides represent a step forward towards the development of more rigid, biochemical stable and active peptides.

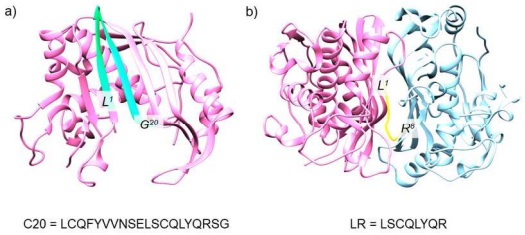

Figure 1. (a) Monomer of hTS taken from PDBid 3N5E. The region corresponding to the **C20** peptide is colored in green. (b) Crystal structure of the complexes of **LR** peptide (in yellow) with hTS (with the two monomers colored in pink and blue, respectively) (PDBid: 3N5E). The protein in the two images has been rotated by 90° around the vertical axis of the image.

RESULTS AND DISCUSSION

Inhibitory activities and conformational propensities. The eight proline derivatives (**[Pro^1]LR** to **[Pro^8]LR**) have been tested against recombinant hTS (Table S1, Figure S1). They showed, at 100 μM, percentages of inhibition between 24% and 56%, similar to their parent peptide LR.[15] **[Pro^2]LR** is the most active among proline mutants.

The propensity of a peptide to assume a secondary structure in the proximity of a target protein molecule reduces the entropic penalty associated with the loss of translational degrees of freedom due to complexation with the protein, and usually increases its affinity for the target and thus its activity.[19] To investigate the conformational propensities behind the biological activities of these peptides, we performed MD simulations and CD experiments. 20 ns MD simulations were run on peptides **[Pro^2]LR** and **[Pro^6]LR**, taken as cases representative of Pro-mutated octapeptides carrying in their sequence a proline residue near the N and the C terminus, respectively. The two mutated peptides in the MD equilibrated complexes with hTS showed structural similarities with the **LR** reference peptide in the crystal structure of the complex with hTS (Figure 2).[19] For all of them, the conformation of the N-terminus region was extended. Given the absence of intra-peptide hydrogen bonding interactions, this portion is disordered in all peptides, though less likely for **[Pro^2]LR.** The decrease in the inner degrees of freedom of this peptide is indeed due to the presence of the proline cycle at position 2. On the other hand, **LR**, **[Pro^2]LR** and **[Pro^6]LR** exhibited turns that involved the residues near the C terminus, and at least two of them showed intramolecular hydrogen bonds. Within peptide **[Pro^6]LR**, only CO(Gln^4) and NH(Gln^7) were hydrogen bonded to each other. This likely stabilizes a distorted β-turn that includes the Pro^6 residue. On the contrary, intramolecular hydrogen bonds between CO(Gln^4) and NH(Gln^7) as well as between CO(Arg^8) and the two NH(Cys^3) and NH(Gln^4) in the **[Pro^2]LR** derivative promote the formation of a compact helical turn. Notably in the crystallographic structure of its complex with hTS, the **LR** peptide exhibits a longer extended portion that involves residues from Leu^1 to Leu^5, while a turn involves only the last three residues at the C terminus. Consistently, no intramolecular hydrogen bond could be identified; only CO(Leu^5) and NH(Gln^7) were within hydrogen bond distance, but in an unfavorable orientation (N-H-O angle = 115°).

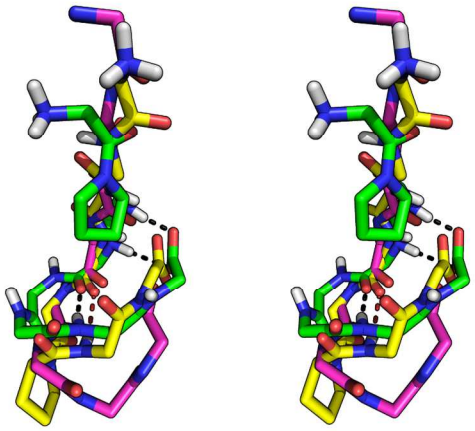

Figure 2. Stereo view of the superimposition of peptides **LR**, **[Pro^2]LR** and **[Pro^6]LR**. The figure combines the X-ray diffraction structure of peptide **LR** (PDBid 3N5E; C atoms of the backbone in magenta) and the 20 ns MD structures of the **[Pro^2]LR** (C atoms of the backbone in green) and **[Pro^6]LR** (C atoms of the backbone in yellow) peptides in their complexes with hTS (PDBid 3N5E). N atoms are shown in blue, O in red, H in white. For clarity purposes, only the backbones and the prolines side chains of the peptides are shown. The black and dark-red dotted lines represent hydrogen bonds in **[Pro^2]LR** and **[Pro^6]LR**, respectively.

These findings provide clues for interpreting the CD spectra of peptides **[Pro^1]LR** to **[Pro^7]LR** obtained in distilled deionized water (DDW), in a 1:4 v/v mixture of DDW and trifluoroethanol (TFE) and in TFE, a solvent known to induce ordered secondary structures (Figures 3 and S2). We simulated the measured spectra as linear combinations of the CD signatures of several secondary structural motifs (Figure S3, Table S2). Contributions from unordered regions, characterized by negative bands with minima around 198 nm, dominate the spectra of all peptides in water. The spectra of all of them except **[Pro^6]LR** feature a positive band between 220 and 235 nm attributable to an electric-dipole allowed tyrosine transition that couples with chiral backbone transitions.[27]

Consistently with the MD structural information on **[Pro^6]LR**, contributions from a type IB-β-turn as well as an unordered region account for the spectra observed for the peptides **[Pro^6]LR** and **[Pro^7]LR** in TFE, where the effect of TFE as a structure-inducing medium is rather weak. The spectra of peptides **LR**, **[Pro^1]LR**, **[Pro^2]LR** and **[Pro^3]LR** in TFE show similar shapes, with a positive band with maximum near 196 nm and two negative bands with minima near 206 and 227 nm. Our attempts to simulate them in terms of standard spectra for secondary structural motifs met with poor results. However, consistent with MD structural findings, the above features are reminiscent of the CD spectrum of a 3(10)-helix.[28] We therefore simulated the spectra of these peptides as combinations of the spectrum of **[Pro^3]LR** in TFE, assumed to correspond to a 3(10)-helix spectrum, and those of the other structural motifs in Figure S2. The results in Table S2 suggest a strong similarity among the structural propensities of the four above mentioned peptides, with a pronounced structure-inducing effect of TFE and only a minor tendency to increased disorder as the mutated position moves towards the N terminus. Finally, the spectra of the peptides that have proline at central positions, **[Pro^4]LR** and **[Pro^5]LR**, show similarities with the spectra of the peptides mutated near the N and the C terminus, i.e., a positive band with maximum at 199 nm, about 3 nm to the red of the 3(10)-helix bands of peptides **[Pro^1]LR** to **[Pro^3]LR**, and a broad negative band that extends towards 240 nm. To simulate them, we had to combine contributions from three different β-turn structural motifs, thus suggesting for these peptides a β-turn-like structures, consistent with the presence of a rigidifying residue such as proline at positions 4 and 5.

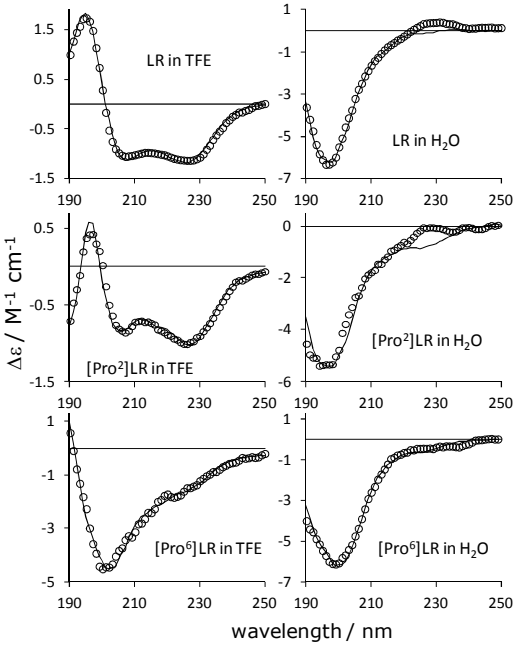

Figure 3. CD spectra of peptides **LR**, **[Pro^2]LR** and **[Pro^6]LR** in water and TFE (circles) and their simulation as combinations of secondary structural motif CD signatures (solid lines).

Overall, mutation to proline at positions 5 and, especially, 6 and 7 generates peptides with lower propensities to assume ordered secondary structures in TFE. The spectra in TFE and the solvent mixture suggest that the peptides that bear proline near the N terminus are more ordered and, taking a 3(10)-type helical conformation rather than a β-turn-like conformation, are likely more compact than the peptides mutated near the C terminus. This suggestion is supported by calculations addressing the rigidness of the two peptides representative of the insertion of proline near the N and C terminus, **[Pro^2]LR** and **[Pro^6]LR,** as well as their compactness (Figure 4). The root-mean-square deviation (RMSD) of the backbone C-alpha atoms of the two Pro-peptides during the first 3ns of the MD simulations were 0.03 ± 0.01 nm (Figure 4a). In **[Pro^2]LR**, the value of the RMSD remained stable in the first 12 ns of simulation and increased to 0.04 ± 0.01 nm in the last 8 ns of simulation. The RMSD value of **[Pro^6]LR** showed a wider fluctuation, raising up to 0.12 ± 0.02 nm between 5 and 12 ns of simulation, and stabilizing to a value of 0.075 ± 0.01 nm in the last 8 ns. This result confirms that **[Pro^2]LR** is more rigid than **[Pro^6]LR**. Noteworthy **[D-Gln^4]LR**, a peptide more active and ordered than the parent **LR**, exhibited an RMSD 0.075 ± 0.02 nm, similar to **[Pro^6]LR**.[29] The calculated radius of gyration in Figure 4b suggests that **[Pro^6]LR** is characterized by a larger surface area than **[Pro^2]LR**. More specifically, while the radius of gyration of **[Pro^2]LR** was stably around 0.43 nm, the radius of gyration calculated for **[Pro^6]LR** increased from 0.45 nm at 3 ns to 0.53 nm at 12 ns, and then it remained 0.47 ± 0.02 nm in the last 8 ns. Once again, this is quite similar to the 0.48-0.49 nm gyration radius found for **[D-Gln^4]LR**.

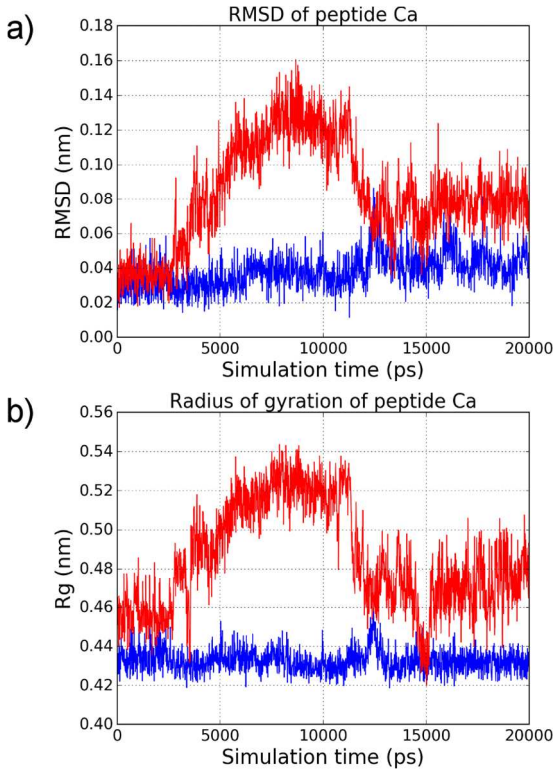

Figure 4. (a) RMSD calculated for the Cα carbon atom positions of the three peptides: **[D-Gln^4]LR** (in black), **[Pro^6]LR** (in red) and **[Pro^2]LR** (in blue). (b) Radius of gyration (Rg) calculated for the two peptides, **[Pro^6]LR** (in red) and **[Pro^2]LR** (in blue). MD simulations were performed on peptides in their complexes with hTS (PDBid 3N5E).

The peptides carrying the proline mutation near the N terminus are slightly more ordered than the peptides with proline near the C terminus. These inferences likely stem from the rigidifying effect of the mutation in the extended and conformationally looser region at the N terminus. However, this decrease in disorder is intrinsic and is expected to occur both in

the free and in the bound peptide; thus, it is not expected to generate any entropy-related gain in affinity towards hTS. In conclusion, the propensity of the peptides **[Pro^1]LR** to **[Pro^7]LR** to arrange residues from 3 to 7 in a compact turn, either of β or of 3(10)-helical types, likely correlates with their similar activities versus hTS, as the inverted cone geometry of the hTS monomer-monomer interface binding region provides optimum space for such compact turns. (Figure S4).

Biological activity. For cancer cell growth inhibition studies we selected three human ovarian carcinoma cell lines, 2008 (cisplatin-sensitive), C13*(cisplatin-resistant phenotype showing high expression levels of the folate-cycle enzymes, TS and DHFR[24]) and IGROV-1 (cisplatin-sensitive), because ovarian cancer tissue is among those with the highest levels of TS expression linked to drug sensitivity.[20] Peptides **[Pro^1]LR** to **[Pro^7]LR** were tested against the above cancer cell models using the SAINT-PhD delivery system. **[Pro^3]LR**, **[Pro^4]LR** and **[Pro^7]LR** resulted to be the most active ones (Figure 5a and Table S3). The percentages of cell viability were calculated by comparing cell cultures exposed to the peptides for 72h versus untreated control cultures. Their effectiveness were compared with those of the lead peptides, **LR** and **[D-Gln^4]LR**, as well as that of **5FU**, taken as a reference drug. The cisplatin-sensitive cell line 2008 showed the greatest sensitivity to all tested peptides, its survival being about 20-25% lower than that of the cisplatin-resistant counterpart, the C13* cells, and of the IGROV-1 cells (Figure 5a). The IC_{50} values of the [Pro^n]- peptides are in the range 0.96-1.57 μM towards 2008 cells (orange histograms in Figure 5b) and in the ranges 3.55-8.1 μM and 4.32-12.1 μM towards C13* (grey histograms) and IGROV-1 (yellow histograms) cells, respectively. With respect to **LR** and **5FU**, the [Pro^n]-peptides showed improved growth inhibition on 2008 cells (IC_{50} = 0.96-1.57 μM vs 4.6 and 6 μM), and a slightly, but consistently better growth inhibition on C13*cells (IC50 = 3.55-8.1 μM vs 9.5 and 12.1 μM growth inhibition compared to **LR** and **5FU** (IC_{50} values are in the range 3.55-8.1 μM for proline mutated peptides and 9.5 and 12.1). Finally **[Pro^3]LR** and **[Pro^7]LR** showed better growth inhibition than **5FU** and **LR** on IGROV-1 cells (IC_{50} = 6.2, 4.32, 10.6 and 8.2 μM, respectively for **[Pro^3]LR**, **[Pro^7]LR**, **LR** and **5FU**). We reason that the overall improved cytotoxicity of the [Pro^n]-peptides relative to the parent **LR** peptide could be ascribed to the proline pyrrolidine ring limiting the conformational freedom of the LR analogues and generating a secondary amide bond in the peptide backbone able to reduce their susceptibility to peptidase action.[30-31]

Thus, the general higher cytotoxic effect of the [Pro^n]- peptides with respect to **LR** and in particular the effect on 2008 cells could be in part explained by an increase in the half-life of the peptides in the cell assay conditions.

To verify a possible correlation between cytotoxicity and intracellular TS inhibition, we evaluated the effects of **[Pro^3]LR**, **[Pro^4]LR** and **[Pro^7]LR** on the TS activity of IGROV-1 cells.[32] Following incubation with **[Pro^3]LR** and **[Pro^4]LR** at 5μM, the intracellular TS activity decreased by 25%, a result similar to that of 5FU at the same concentration. On the other hand, at the same concentration, **[Pro^7]LR** inhibited the enzyme activity by more than 30% (Figure 5b, Table S3, Figure S5). **LR** showed a similar effect against 2008 and C13* cell lines (TS activity decreased in the range 20-40% at 10 or 20 μM).[19] Thus, the observed inhibition of intracellular TS activity by the three peptides confirms that TS is one of the target of the here described peptides.

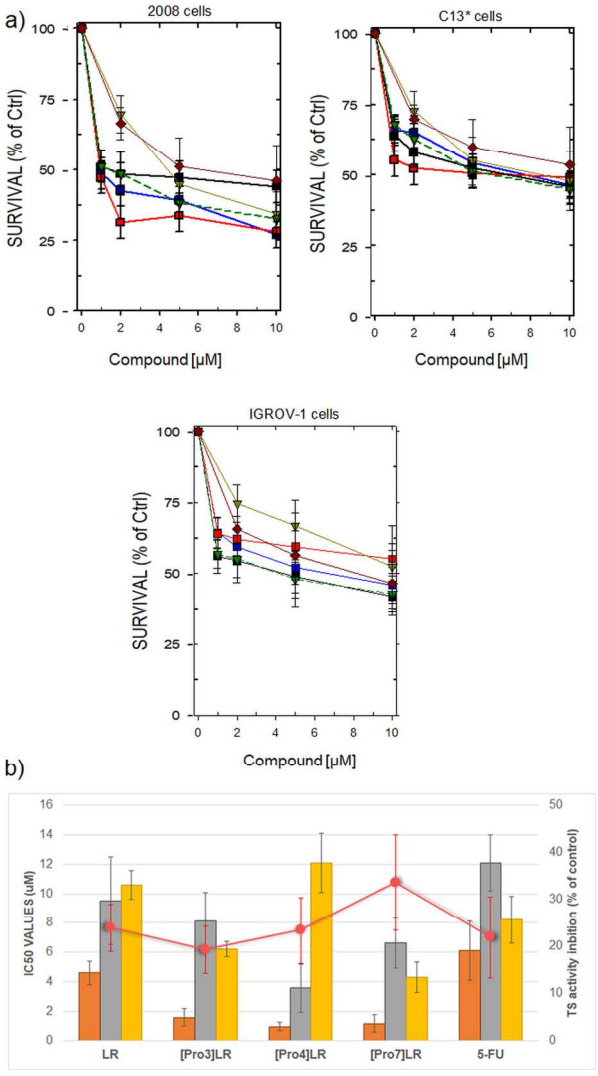

Figure 5. (a) Dose-response curve of 2008, C13* and IGROV-1 cell growth after 72 h exposure to **[Pro^3]LR** (blue squares), **[Pro^4]LR** (red squares), **[Pro^7]LR** (black squares), **5FU** (dark red diamonds), **LR** (golden triangles down), **[D-Gln^4]LR** (green triangles down). Cell survival percentages are the mean ± S.E.M. of three separate experiments performed in duplicate. (b) The combo graph of the percentage of TS activity inhibition in IGROV-1 cells treated for 72 hr (red scatter graph) and IC_{50} against 2008 (orange histograms), C13* (gray histograms) and IGROV-1 (yellow histograms) human ovarian cancer cell lines. For the percentage of TS activity inhibition IGROV-1 cells were treated with 5μM of 5FU or peptides (transfected by SAINT-PhD system). Percentage are calculated by comparison with the TS activity in IGROV-1 cells untreated, used as control. For **LR,** it is reported the value against 2008 cells at 10 μM.[19] TS activity inhibition percentage and IC_{50} values are the mean ± S.E.M of three independent experiments.

Evaluation of protein expression associated with peptides inhibition activity. For a deeper exploration of the cellular

mechanism of these peptides, the evaluation of the protein set modulation associated with their activity was analyzed. A quantitative analysis of the expression of proteins TS, DHFR, TRAP, and HSP90 has been carried out on IGROV-1 cancer cells following treatment with peptides **[Pro^3]LR** and **[Pro^4]LR**. **PMX** was considered as drug of reference because it binds to hTS active site and it shows a well known inhibition mechanism[9,15]. The analysis was performed via western blot and results compared with the results previously obtained with the lead **LR** and **[D-Gln^4]LR**.[15] The changes in the expression levels of the four proteins after treatment with **PMX** and with peptides **[D-Gln^4]LR**, **[Pro^3]LR** and **[Pro^4]LR** are shown in Figures 6 and S6. The quantitative data were represented through heat-map (Figure 6a) and histograms respectively, thus giving a comprehensive visualization of the changes.

The results obtained in the treatments with the peptides showed that proteins TS, DHFR and HSP90 were similarly modulated in IGROV-1 cells. TS is the known target of **LR** and its derivatives while DHFR is the second enzyme in the thymidylate cycle. **PMX** caused a modulation of the expressions of these three proteins different from those of the three peptides. Similar results have been observed in comparison with **LR** and also in other cell lines.[15] **[Pro^4]LR** showed the typical protein profile defined for **LR** and **[D-Gln^4]LR**.[15] **[Pro^3]LR** exhibits the same trend as **[Pro^4]LR**, except for TRAP1, a mitochondrial chaperone associated with chemoresistant and anti-apoptotic phenotypes,[33] that shows an unexpected up regulation with respect to the control. TRAP1 was down regulated by **[Pro^4]LR** and **[D-Gln^4]LR** in IGROV-1 cells and the same behavior was detected also with **LR** in IGROV-1 and other cell lines.[15] We performed a statistical analysis of the results to assess the significance of the observed changes. The modulation of each protein expressions by each cell treatment is represented in the boxplots of Figure 6b. The highest modulation of expression levels is observed for TS and DHFR after treatment with **PMX** (TS.PMX and DHFR.PMX couples median =3.0 and 4,7, mean =3.1 and 4.8, respectively). All the other pairs have median and mean expression values lower than 1.5. Thus, treatment with **PMX** produces the strongest data difference effect. The analysis points out that **PMX** and the peptides have different proteins set expression. We interpret this difference as a consequence of different mechanisms of hTS inhibition that is then translated in a different behavior at the cellular level, as previously highlighted by a comparison between **LR, [D-Gln^4]LR** and **PMX** [15] and the similarity between the proline mutated peptides and the leads.

CONCLUSIONS

We have discovered two derivatives, **[Pro^3]LR** and **[Pro^4]LR**, showing stronger inhibition on ovarian cancer cell growth with respect to the lead peptide **LR**, better than or comparable with **5FU**. CD spectroscopic evidence on the investigated [Pro^n]-peptides, supported by the MD simulations performed on **[Pro^6]LR** and **[Pro^2]LR**, has shown conformational propensities similar to those of **LR** and its more rigid and active derivative, **[D-Gln^4]LR**, but more compact shapes. A similarity between the inhibition of the catalytic activity of the recombinant protein and of the intracellular TS activity is observed, thus supporting the hypothesis that the observed effect on cancer cells is attributable, at least partially, to hTS inhibition.

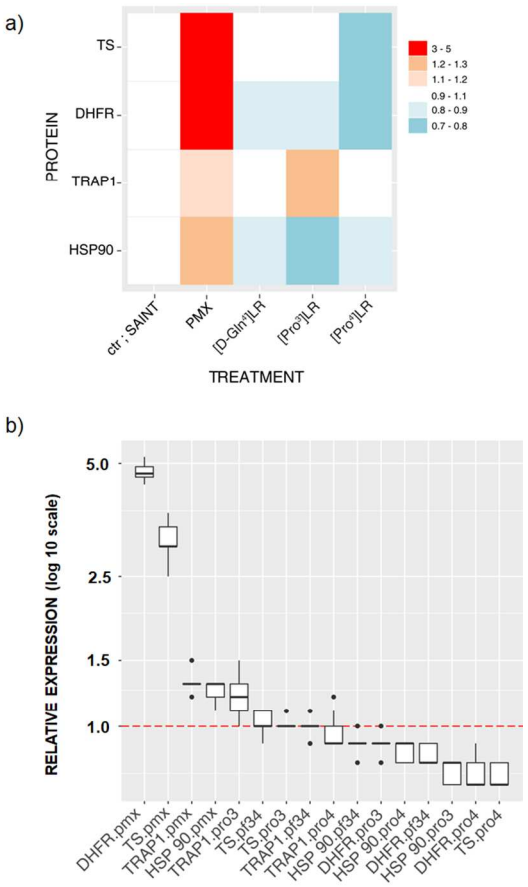

Figure 6. (a) Heat map of the protein expression modulation profile of the tested compounds in IGROV-1 human cisplatin-sensitive ovarian cancer cell line. Each expression value is standardized by subtracting the corresponding value in the control sample (ctr or SAINT). The scale in the legend illustrates the extent of up (red)- and down (green)-regulation. (b) Boxplot representation of the expression level modulation of each protein (HSP90, TRAP1, TS, DHFR) due to each treatment (**[Pro^3]LR**, **[Pro^4]LR**, **[D-Gln^4]LR** and **PMX**). The labels along the x-axis are composed in the format "protein.treatment" and the boxplots are ordered according to decreasing median values. The horizontal dashed red line at y=1.0 represents the control samples (ctr or SAINT).

ANOVA test using the multiple comparisons method of Tukey-HSD (Honest Significant Differences) (Figure S7) definitely confirmed the results obtained with the statistical analysis.

Like **LR** and **[D-Gln^4]LR**, these peptides do not induce intracellular hTS overexpression and cause modulation of a proteins set that is similar to that observed for the two reference octapeptides,[15] and statistically significantly different from that obtained with **PMX**. This provides further support to the claim that the cellular mechanism of action is similar for all the studied peptides, but different from that of **PMX**. Notably the introduction of proline likely stabilizes the peptides *vs* the peptidase degradation, thus increasing their intracellular concentration and activity. For all the mentioned reasons, the LR proline analogs represent a step forward towards the identification of more active and metabolically stable anticancer peptides. These peptides may show a broader cancer cell inhibition activity also against those cancer cells expressing high hTS levels such as nasopharynge[25] and human gastrointen-

stinal cancer cells[26] from patients treated with cisplatin- and 5FU-based chemotherapy.

EXPERIMENTAL SECTION

General. Amino acid derivatives, reagents, and solvents were purchased from Sigma Aldrich (Steinheim, Germany) or Bachem (Bubendorf, Switzerland). The purity of the tested compounds has been assessed by reverse-phase high-performance liquid chromatography (RP-HPLC). All compounds showed >95% purity. Exact mass was recorded with an Agilent ESI-Q-TOF 6520 instrument.

Peptide synthesis. All peptides were synthesized with an automatic solid phase peptide synthesizer Syro II (Biotage, Uppsala Sweden) using Fmoc/tBu chemistry.[34] A preloaded 4-Benzyloxybenzyl alcohol resin (Wang resin) was used as a solid support for the synthesis of LR derivatives replaced with Pro in position 1 to 7 while **[Pro^8]LR** was obtained starting from H-Pro-2-chlorotrityl resin, a solid support useful to minimize diketopiperazine formation.[35] The Fmoc protecting group was removed by treatment with 40% v/v piperidine/dimethylformamide (DMF). All the Fmoc amino acids (4 equiv) were coupled to the growing peptide chain by using HATU (4 equiv) in DMF in the presence of an equimolar concentration of 4-methylmorpholine (NMM), and the coupling reaction time was 1h. To improve the analytical profile of the crude peptide, capping with 3:1 v/v acetic anhydride (0.5M in DMF) and NMM (0.25M in DMF), 2mL/0.2 g of resin, was performed at each step. The protected peptide-resin was treated with reagent B[36] (trifluoroacetic acid (TFA)/H_20/ phenol/triiso-propylsilane 88:5:5:2; v/v; 10 mL/0.2 g of resin) for 2h at room temperature. After filtration of the resin, the solvent was evaporated in vacuo and the residue triturated with ether. Crude peptides were purified by preparative reverse phase HPLC to yield a white powder after lyophilization.

Peptide Purification. Crude peptides were purified by preparative reversed-phase HPLC using a Water Delta Prep 3000 system with a Jupiter column C18 (250 x 30 mm, 300 angstrom, 15 mm spherical particle size). The column was perfused at a flow rate of 20 mL/min with a mobile phase containing solvent A (0.1% TFA in DDW), and a linear gradient from 5 to 50% of solvent B (60%, v/v, acetonitrile/0.1% TFA in DDW) over 25 min for the elution of peptides. Analytical HPLC analyses were performed on a Beckman 116 liquid chromatograph equipped with a Beckman 166 diode array detector. Analytical purity of the peptides were determined using a Luna C18 column (4.6 x 100 mm, 3 μm particle size) with the above solvent system (solvents A and B) programmed at a flow rate of 0.5 mL/min using a linear gradient from 0% to 80% B over 25 min. All analogues showed ≥ 95% purity when monitored at 220 nm. Accurate mass of final compounds were determined using an Agilent 6520 ESI/Q-TOF mass spectrometer and the data obtained are reported as supporting information (Figures S8-S23).

hTS purification and enzymatic assay. hTS was purified as previously reported.[37] Protein inhibition studies were performed as already reported.[18] Details are reported in the Supplementary Information.

CD studies. All CD spectra were measured with a Jasco spectropolarimeter. Each spectrum is the average of 2-6 acquisitions. Experiments were performed as already reported[11]. More details are reported in Supplementary Information.

MD simulations. MD simulations were conducted with the software GROMACS[38] applying parameters and protocols as already reported for previously studied similar systems.[27] Details are reported in the Supplementary Information.

Cell line growth and cytotoxicity evaluation. 2008, C13*, and IGROV-1 human ovarian carcinoma cell lines were grown in RPMI 1640 medium (Lonza) containing 10% heat-inactivated fetal bovine serum. The cells were incubated at 37°C under 5% CO_2 for at least 24h before treatment with the peptides. Treatments were performed as already reported.[24] Details are reported in Supplementary Information.

Cellular TS activity evaluation. The catalytic activity of TS after cell incubation with proline mutated LR peptides was determined by measuring the amounts of ^{3}H released during the TS catalyzed conversion of [5-^{3}H]dUMP to dTMP.[32] Details are reported in the Supplementary Information.

Protein extraction and Western Blot analysis for protein semi-quantification. Identification and semi-quantification of TS, DHFR, TRAP1 and HSP90 has been performed as already reported.[16] Details on the protein extraction, molecular biology and western blot analysis are reported in the Supplementary Information.

Statistical analysis. Details are reported in Supplementary Information.

ASSOCIATED CONTENT

Supporting Information. Peptide percentage of inhibition of recombinant hTS, CD spectra of [Pro1]LR - [Pro7]LR, CD spectra of secondary structure motifs, contributions of CD signatures of secondary structural motifs in the simulation of the CD spectra of peptides [Pro1]LR to [Pro7]LR, the peptide binding site, proline mutated LR peptides IC_{50} values against 2008, C13* and IGROV-1 cell lines, inhibition of cellular TS activity in IGROV-1 cells, comparison of expression levels modulation by pair of treatments, protein expression modulation profile of the tested compounds in IGROV-1 human cisplatin-sensitive ovarian cancer cell line, HPLC profiles of peptide characterization, experimental section details, PDB files of the two complexes, hTS in complex with [Pro^2]LR and [Pro^6]LR, from MD studies. This material is available free of charge via the Internet at http://pubs.acs.org.

AUTHOR INFORMATION

Corresponding Authors

* Prof. Maria Paola Costi. Phone: 0039-059-2058579; email: mariapaola.costi@unimore.it
* Prof. Glauco Ponterini. Phone: 0039-059-2058593; email: glauco.ponterini@unimore.it

Present Addresses

Puneet Saxena. Excelra Knowledge Solutions Pvt. Ltd., 6th floor, Wing B, NSL SEZ Arena, Plot No. 679, Survey No. 1, IDA UppalMallapur, Nacharam, Hyderabad-50003976 India.
$ Chiara Marraccini. Transfusion Medicine Unit, ASMN-IRCCS Reggio Emilia, Italy.

Author Contributions

The manuscript was written through contributions of all authors. All authors have given approval to the final version of the manuscript.

Funding Sources

This work was financially supported by the Italian Association for Cancer Research (IG 10474 and IG 16977 to M.P.C.).

ACKNOWLEDGMENT

The authors acknowledge Prof. Els Berns of the Erasmus Institute, Rotterdam, for making the IGROV-1 cell line available. This research benefits from the HPC (High Performance Computing) facility of the University of Parma, Italy - http://www.hpc.unipr.it.

ABBREVIATIONS

5FU, 5-fluorouracil; CD, circular dichroism; DDW, distilled deionized water; DHFR, dihydrofolate reductase; DMF, dimethylformamide; DMSO, dimethyl sulphoxide; dUMP, 2'-deoxyuridine-5'-monophosphate; HSP90, heat shock protein HSP 90-alpha; hTS, human thymidylate synthase; IC_{50}, inhibitor concentration reducing enzyme activity of 50% or inhibitor concentration able to reduce cell line growth of 50%; Km, Michaelis-Menten constant; MD, molecular dynamics; mTHF, N5,N10methylentetra-hydrofolate; PMX, pemetrexed; RMSD, root-mean-square deviation; TFA, trifluoroacetic acid; TFE, trifluoroethanol; TRAP1, heat shock protein 75 kDa, mitochondrial; TS, thymidylate synthase.

REFERENCES

(1) Chu, E.; Allegra, C. J. The role of thymidylate synthase as an RNA binding protein. *BioEssays* **1996**, *18*, 191–198.

(2) Chu, E.; Koeller, D. M.; Casey, J. L.; Drake, J. C.; Chabner, B. A.; Elwood, P. C.; Zinn, S.; Allegra, C. J. Autoregulation of human thymidylate synthase messenger RNA translation by thymidylate synthase. *Proc. Natl. Acad. Sci. U. S. A.* **1991**, *88*, 8977–8981.

(3) Chu, E.; Voeller, D.; Koeller, D. M.; Drake, J. C.; Takimoto, C. H.; Maley, G. F.; Maley, F.; Allegra, C. J. Identification of an RNA binding site for human thymidylate synthase. *Proc. Natl. Acad. Sci. U. S. A.* **1993**, *90*, 517–521.

(4) Liu, J.; Schmitz, J. C.; Lin, X.; Tai, N.; Yan, W.; Farrell, M.; Bailly, M.; Chen, T. min; Chu, E. Thymidylate synthase as a translational regulator of cellular gene expression. *Biochim. Biophys. Acta* **2002**, *1587*, 174–182.

(5) Carreras, C. W.; Santi, D. V. The catalytic mechanism and structure of thymidylate synthase. *Annu. Rev. Biochem*. **1995**, *64*, 721–762.

(6) Stroud, R. M.; Finer-Moore, J. S. Conformational dynamics along an enzymatic reaction pathway: thymidylate synthase, "the movie." *Biochemistry (Mosc.)* **2003**, *42*, 239–247.

(7) Finer-Moore, J. S.; Santi, D. V.; Stroud, R. M. Lessons and conclusions from dissecting the mechanism of a bisubstrate enzyme: thymidylate synthase mutagenesis, function, and structure. *Biochemistry (Mosc.)* **2003**, *42*, 248–256.

(8) Jackman, A. L.; Taylor, G. A.; Gibson, W.; Kimbell, R.; Brown, M.; Calvert, A. H.; Judson, I. R.; Hughes, L. R. ICI D1694, a quinazoline antifolate thymidylate synthase inhibitor that is a potent inhibitor of L1210 tumor cell growth in vitro and in vivo: a new agent for clinical study. *Cancer Res.* **1991**, *51*, 5579–5586.

(9) Shih, C.; Chen, V. J.; Gossett, L. S.; Gates, S. B.; MacKellar, W. C.; Habeck, L. L.; Shackelford, K. A.; Mendelsohn, L. G.; Soose, D. J.; Patel, V. F.; Andis, S. L.; Bewley, J. R.; Rayl, E. A.; Moroson, B. A.; Beardsley, G. P.; Kohler, W.; Ratnam, M.; Schultz, R. M. LY231514, a pyrrolo[2,3-d]pyrimidine-based antifolate that inhibits multiple folate-requiring enzymes. *Cancer Res.* **1997**, *57* (6), 1116–1123.

(10) Sayre, P. H.; Finer-Moore, J. S.; Fritz, T. A.; Bier-mann, D.; Gates, S. B.; MacKellar, W. C.; Patel, V. F.; Stroud, R. M. Multi-targeted antifolates aimed at avoiding drug resistance form covalent closed inhibitory complexes with human and Escherichia coli thymidylate synthases. *J. Mol. Biol.* **2001**, *313*, 813–829.

(11) Cardinale, D.; Salo-Ahen, O. M. H.; Ferrari, S.; Ponterini, G.; Cruciani, G.; Carosati, E.; Tochowicz, A. M.; Mangani, S.; Wade, R. C.; Costi, M. P. Homodimeric enzymes as drug targets. *Curr. Med. Chem.* **2010**, *17*, 826–846.

(12) de Vega, M. J. P.; Martín-Martínez, M.; González-Muñiz, R. Modulation of protein-protein interactions by stabilizing/mimicking protein secondary structure elements. *Curr. Top. Med. Chem.* **2007**, *7*, 33–62.

(13) Fletcher, S.; Hamilton, A. D. Targeting protein-protein interactions by rational design: mimicry of protein surfaces. *J. R. Soc. Interface* **2006**, *3*, 215–233.

(14) Loregian, A.; Palù, G. Disruption of protein-protein interactions: towards new targets for chemotherapy. *J. Cell. Physiol.* **2005**, *204*, 750–762.

(15) Pelà, M.; Saxena, P.; Luciani, R.; Santucci, M.; Ferrari, S.; Marverti, G.; Marraccini, C.; Martello, A.; Pirondi, S.; Genovese, F.; Salvadori, S.; D'Arca, D.; Ponterini, G.; Costi, M. P.; Guerrini, R. Optimization of peptides that target human thymidylate synthase to inhibit ovarian cancer cell growth. *J. Med. Chem.* **2014**, *57*, 1355–1367.

(16) Ponterini, G.; Martello, A.; Pavesi, G.; Lauriola, A.; Luciani, R.; Santucci, M.; Pelà, M.; Gozzi, G.; Pacifico, S.; Guerrini, R.; Marverti, G.; Costi, M. P.; D'Arca, D. Intracellular quantitative detection of human thymidylate synthase engagement with an unconventional inhibitor using tetracysteine-diarsenical-probe technology. *Sci. Rep.* **2016**, *6*, 27198, doi: 10.1038/srep27198.

(17) Genovese, F.; Gualandi, A.; Taddia, L.; Marverti, G.; Pirondi, S.; Marraccini, C.; Perco, P.; Pelà, M.; Guerrini, R.; Amoroso, M. R.; Esposito, F.; Martel-lo, A.; Ponterini, G.; D'Arca, D.; Costi, M. P. Mass spectrometric/bioinformatic identification of a protein subset that characterizes the cellular activity of anticancer peptides. *J. Proteome Res.* **2014**, *13*, 5250–5261.

(18) Tochowicz, A.; Santucci, M.; Saxena, P.; Guaitoli, G.; Trande, M.; Finer-Moore, J.; Stroud, R. M.; Costi, M. P. Alanine mutants of the interface residues of human thymidylate synthase decode key features of the binding mode of allosteric anticancer peptides. *J. Med. Chem.* **2015**, *58*, 1012–1018.

(19) Cardinale, D.; Guaitoli, G.; Tondi, D.; Luciani, R.; Henrich, S.; Salo-Ahen, O. M. H.; Ferrari, S.; Mar-verti, G.; Guerrieri, D.; Ligabue, A.; Frassineti, C.; Pozzi, C.; Mangani, S.; Fessas, D.; Guerrini, R.; Ponterini, G.; Wade, R. C.; Costi, M. P. Protein-protein interface-binding peptides inhibit the cancer therapy target human thymidylate synthase. *Proc. Natl. Acad. Sci.* **2011**, *108*, E542–E549.

(20) Qing, L.; Boyer, C.; Lee, J. Y.; Shepard, H. M. A novel approach to thymidylate synthase as a target for cancer chemotherapy. *Mol. Pharmacol.* **2001**, *59*, 446-452.

(21) Scanlon, K. J.; Kashani-Sabet, M. Elevated expression of thymidylate synthase cycle genes in cisplatin-resistant human ovarian carcinoma A2780 cells. *Proc Natl Acad Sci U S A.* **1988**, *85*, 650-653.

(22) Lu, Y.; Han, J.; Scanlon, K. J. Biochemical and molecular properties of cisplatin-resistant A2780 cells grown in folinic acid. *J Biol Chem.* **1988**, *263*, 4891-4894.

(23) Newman, E. M.; Lu, Y.; Kashani-Sabet, M.; Kesavan, V.; Scanlon, K. J. Mechanisms of cross-resistance to methotrexate and 5-fluorouracil in an A2780 human ovarian carcinoma cell subline resistant to cisplatin. *Biochem Pharmacol.* **1988**, *37*, 443-447.

(24) Marverti, G.; Ligabue, A.; Paglietti, G.; Corona, P.; Piras, S.; Vitale, G.; Guerrieri, D.; Luciani, R.; Costi, M.P.; Frassineti, C.; Moruzzi, M.S.. Collateral sensitivity to novel thymidylate synthase inhibitors correlates with folate cycle enzymes impairment in cisplatin-resistant human ovarian cancer cells. *Eur J Pharmacol*. **2009**, *615*, 17-26.

(25) Hwang, Y.; Lee, H.; Jeong, J.; Kang, S.; Ahn, M.; Han, J.; Kim, J.; Kim, C.; Choi. , J. Expression of drug-resistance-related proteins in nasopharyngeal cancer (NPC) patients treated with cisplatin-based concurrent chemoradiotherapy. *J. Clin. Oncology* **2010**, *28*, 5551-5551)

(26) Nishiyama, M.; Yamamoto, W.; Park, J.-S.; Okamoto, R.; Hanaoka, H.; Takano H.; Saito, N.; Matsukawa, M.; Shirasaka, T.; Kurihara, M.. Fluorouracil in Combination Can Repress Increased Gene Expression of Cellular Resistance Determinants to Themselves. *Clin. Cancer Res.* **1999**, *5*, 2620–2628).

(27) Sreerama, N.; Manning, M. C.; Powers, M. E.; Zhang, J. X.; Goldenberg, D. P.; Woody, R. W. Tyrosine, phenylalanine, and disulfide contributions to the circular dichroism of proteins: circular dichroism spectra of wild-type and mutant bovine pancreatic trypsin inhibitor. *Biochemistry (Mosc.)* **1999**, *38*, 10814–10822.
(28) Andersen, N. H.; Liu, Z.; Prickett, K. S. Efforts toward deriving the CD spectrum of a 3(10) helix in aqueous medium. *FEBS Lett.* **1996**, *399*, 47–52.
(29) Mentlein, R. Proline residues in the maturation and degradation of peptide hormones and neuropeptides. *FEBS Lett.* **1988**, *234*, 251–256.
(30) Cunningham, D. F.; O'Connor, B. Proline specific peptidases. *Biochim Biophys Acta.* **1997**, *1343*, 160-186.
(31) Vanhoof, G.; Goossens, F.; De Meester, I.; Hendriks, D.; Scharpé, S. Proline motifs in peptides and their biological processing. *FASEB J.* **1995**, *9*, 736-744.
(32) van Triest, B; Pinedo, H. M.; van Hensbergen, Y; Smid, K.; Telleman, F.; Schoenmakers, P. S.; van del Wilt, C. L.; van Laar, J. A.; Noordhuis, P.; Jansen, G.; Peters, G. J. Thymidylate synthase level as the main predictive parameter for sensitivity to 5-fluorouracil, but not for folate-based thymidilate synthase inhibitors, in 13 nonselected colon cancer cell lines. *Clin Cancer Res* **1999**, *5*, 643-654.
(33) Loizeau, K.; De Brouwer, V.; Gambonnet, B.; Yu, A.; Renou, J.-P.; Van Der Straeten, D.; Lambert, W. E.; Rébeillé, F.; Ravanel, S. A genome-wide and metabolic analysis determined the adaptive response of arabidopsis cells to folate depletion induced by methotrexate. *Plant Physiol.* **2008**, *148*, 2083–2095.
(34) Benoiton, N. L. Chemistry of Peptide Synthesis. Taylor & Francis: New York, 2006; pp 65-90.
(35) Barlos, K.; Gatos, D.; Papaphotiou, G.; Schäfer, W. Synthese von calcitonin-derivaten durch fragmentkondensation in Lösung und am 2-Chlortrityl-Harz. *Liebigs Ann. Chem.* **1993**, *1993*, 215–220.
(36) Sole, N. A.; Barany, G. Optimization of solid-phase synthesis of [Ala^8]-Dynorphin A. *J. Org. Chem.* **1992**, *57*, 5399–5403.
(37) Schiffer, C. A.; Clifton, I. J.; Davisson, V. J.; Santi, D. V.; Stroud, R. M. Crystal structure of human thymidylate synthase: a structural mechanism for guiding substrates into the active site. *Biochemistry (Mosc.)* **1995**, *34*, 16279–16287.
(38) Hess, B.; Kutzner, C.; van der Spoel, D.; Lindahl, E. GROMACS 4: Algorithms for highly efficient, load-balanced, and scalable molecular simulation. *J. Chem. Theory Comput.* **2008**, *4*, 435–447.

Table of Contents